Georg-August-Universität
Göttingen

Local projection stabilization for advection-diffusion-reaction problems: One-level vs. two-level approach

Knobloch, P., Lube, G.

Nr. 2008-13

Preprint-Serie des
Instituts für Numerische und Angewandte Mathematik
Lotzestr. 16-18
D - 37083 Göttingen

LOCAL PROJECTION STABILIZATION FOR ADVECTION-DIFFUSION-REACTION PROBLEMS: ONE-LEVEL VS. TWO-LEVEL APPROACH

P. KNOBLOCH* AND G. LUBE†

Abstract. Local projection stabilization (LPS) of finite element methods is a new technique for the numerical solution of transport-dominated problems. In this paper, a critical discussion and comparison of the one- and two-level approaches to LPS is given for the linear advection-diffusion-reaction problem. Moreover, the relation between the LPS method and residual-based stabilization techniques is explained for simplical elements. June 30, 2008

Key words. Local projection stabilization, finite element method, advection-diffusion-reaction problem, advection-dominated problem, SUPG method.

AMS subject classifications. 65N30, 65N12, 65N15

1. Introduction. Consider the stationary advection-diffusion-reaction problem

$$Lu := -\varepsilon\Delta u + \boldsymbol{b}\cdot\nabla u + \sigma u = f \qquad \text{in } \Omega; \qquad u = 0 \quad \text{on } \partial\Omega \tag{1.1}$$

for the scalar field u in a bounded domain $\Omega \subset \mathbb{R}^d$, $d = 2, 3$, with given source term f, advection field $\boldsymbol{b}$ and constant data $\varepsilon > 0, \sigma \geq 0$. Problem (1.1) is a basic model in fluid mechanics and many other applications.

The Galerkin finite element (FE) approximation of (1.1) may suffer from dominating advection, i.e., $\varepsilon \ll \|\boldsymbol{b}\|_{[L^\infty(\Omega)]^d}$, and/or dominating reaction, i.e., $\varepsilon \ll \sigma$. The traditional way to cope with this problem is the application of residual-based stabilization (RBS) techniques. The basic approach is the streamline-upwind/Petrov-Galerkin (SUPG) method [6] or related variants. An overview about RBS methods can be found in [22].

The class of RBS techniques is still quite popular since they are robust and easy to implement. Nevertheless, they have severe drawbacks stemming from the non-symmetric form of the stabilization terms and the occurence of second-order derivatives in the residual $Lu - f$. Therefore, other stabilization techniques appeared recently, in particular, the edge-stabilization method [7, 5] and variational multiscale (VMS) methods [15, 16, 13, 8]. We emphasize that almost all stabilization methods can be interpreted as special VMS methods. The key idea of VMS methods is a separation of scales: large scales, small scales and unresolved scales. The influence of the unresolved scales on the other scales has to be modelled. Mostly, it is assumed that the unresolved scales do not influence the large scales.

Local projection stabilization (LPS) methods as special VMS-type methods are of current interest [4, 19]. Here the influence of the unresolved scales on the small scales is modelled by additional artificial diffusion terms for the small scales. LPS methods belong to the class of symmetric stabilization techniques [5]. One major advantage of such methods applied to optimization problems with partial differential equations is that the operations 'discretization' and 'optimization' commute [3].

There are currently two basic variants of LPS methods: a two-level approach [4, 19, 21] and a one-level approach [19, 24, 20, 10]. One goal of this paper is a critical review of the numerical analysis (based on energy estimates) and a comparison of both variants. It is another goal of this paper to show that this approach is very close to RBS methods

[1]Charles University, Faculty of Mathematics and Physics, Department of Numerical Mathematics, Sokolovská 83, 186 75 Praha 8, Czech Republic (`knobloch@karlin.mff.cuni.cz`).

[2]Math. Department, NAM, University of Göttingen, Lotzestrasse 16-18, D-37083 Göttingen, Germany (`lube@math.uni-goettingen.de`).

like the algebraic subgrid scale stabilization [14, 8] or the 'unusual' Galerkin/least-squares method [9].

The outline of the paper is as follows. The basic Galerkin FEM and its stabilization via local projection is discussed in Section 2. In Section 3 of this paper, we present a unified theory of local projection methods for problem (1.1) based on energy estimates. In contrast to other papers, the dependence on the polynomial degree of the finite element method is considered. In Section 4, examples of finite element spaces satisfying the assumptions of Section 3 are presented and, in Section 5, a comparison of both variants of LPS methods is performed by means of simple numerical experiments. Section 6 is devoted to the relationship between simplicial LPS methods and residual-based stabilization methods.

Throughout this paper, standard notations for Lebesgue and Sobolev spaces are used. The L^2 inner product in a domain G is denoted by $(\cdot,\cdot)_G$. Moreover, we use the notation $a \lesssim b$ if there exists a constant $C > 0$ independent of all relevant parameters like mesh size, polynomial degree or coefficients of L.

2. Variational formulation and stabilization. Here, the basic Galerkin finite element formulation of problem (1.1) and its stabilized variants via local projection (LPS) are introduced. Moreover, various technical tools are given.

2.1. Basic Galerkin approximation. The variational formulation for the advection-diffusion-reaction problem (1.1) reads: Find $u \in V := H_0^1(\Omega)$ such that

$$a(u,v) := (\varepsilon\nabla u, \nabla v)_\Omega + (\boldsymbol{b}\cdot\nabla u + \sigma u, v)_\Omega = (f,v)_\Omega, \qquad \forall v \in V. \tag{2.1}$$

ASSUMPTION 1. *Let $\Omega \subset \mathbb{R}^d$, $d \in \{2,3\}$, be a bounded, polyhedral domain. Moreover, assume that $\varepsilon > 0$ is constant, $f \in L^2(\Omega)$, $\boldsymbol{b} \in [L^\infty(\Omega) \cap H^1(\Omega)]^d$ with $\nabla\cdot\boldsymbol{b} = 0$ a.e. in Ω and $\sigma \geq 0$ is constant.*

REMARK 1. *Typically, $\boldsymbol{b}$ is a finite element solution of an incompressible flow problem. Then there holds $(\nabla\cdot\boldsymbol{b}, q_h)_\Omega = 0$ for certain test functions q_h. Hence, $\nabla\cdot\boldsymbol{b}$ is small but does not vanish in general. A simple remedy to ensure coercivity of $a(\cdot,\cdot)$ is to replace the advective term $(\boldsymbol{b}\cdot\nabla u, v)_\Omega$ by $\frac{1}{2}(\boldsymbol{b}\cdot\nabla u, v)_\Omega - \frac{1}{2}(\boldsymbol{b}\cdot\nabla v, u)_\Omega - \frac{1}{2}((\nabla\cdot\boldsymbol{b})u, v)_\Omega$.*

Consider a shape-regular, admissible decomposition $\mathcal{T}_h$ of Ω into d-dimensional simplices, quadrilaterals in the two-dimensional case or hexahedra for three dimensions. Let h_T be the diameter of a cell $T \in \mathcal{T}_h$ and h the maximum of all h_T, $T \in \mathcal{T}_h$. Let $\hat{T}$ be a reference element of the decomposition $\mathcal{T}_h$. Let us assume that, for each $T \in \mathcal{T}_h$, there exists an affine mapping $F_T : \hat{T} \to T$ which maps $\hat{T}$ onto T. This quite restrictive assumption for quadrilaterals can be weakened to asymptotically affine mappings [1].

Set $P_{k,\mathcal{T}_h} := \{v_h \in L^2(\Omega)\ ;\ v_h \circ F_T \in P_k(\hat{T})\ , T \in \mathcal{T}_h\}$ with the space $P_k(\hat{T})$ of complete polynomials of degree k defined on $\hat{T}$ and $Q_{k,\mathcal{T}_h} := \{v_h \in L^2(\Omega)\ ;\ v_h \circ F_T \in Q_k(\hat{T})\ , T \in \mathcal{T}_h\}$ with the space $Q_k(\hat{T})$ of all polynomials on $\hat{T}$ with maximal degree k in each coordinate direction. We shall approximate the space V by a finite element space $V_{h,k} \subset V$ such that

$$V_{h,k} \supset P_{k,\mathcal{T}_h} \cap V \quad \text{or} \quad V_{h,k} \supset Q_{k,\mathcal{T}_h} \cap V.$$

Now, the standard Galerkin discretization of problem (1.1) reads: Find $u_h \in V_{h,k}$ such that

$$a(u_h, v_h) = (f, v_h)_\Omega, \qquad \forall v_h \in V_{h,k}. \tag{2.2}$$

As mentioned in the introduction, the solution u_h of (2.2) usually suffers from spurious oscillations, which is often cured by introducing a stabilization in (2.2).

2.2. Local projection stabilization (LPS). The idea of LPS methods is to split the discrete function spaces into small and large scales and to add stabilization terms of diffusion-type acting only on the small scales. There are two obvious choices of the space of large scales: a two-level and a one-level approach.

The first, the two-level variant, is to determine the large scales with the help of a coarse mesh. The coarse mesh $\mathcal{M}_h$ is constructed by coarsening the basic mesh $\mathcal{T}_h$ such that each macro-element $M \in \mathcal{M}_h$ is the union of one or more neighbouring cells $T \in \mathcal{T}_h$. The diameter of $M \in \mathcal{M}_h$ is denoted by h_M. We assume that the decomposition $\mathcal{M}_h$ of Ω is non-overlapping and shape-regular. Additionally, the interior cells are supposed to be of the same size as the corresponding macro-cell:

$$\exists\, C > 0 \ : \quad h_M \le C h_T, \quad \forall T \in \mathcal{T}_h, M \in \mathcal{M}_h \text{ with } T \subset M. \tag{2.3}$$

Following the approach in [19], we define a discrete space $D_h \subset L^2(\Omega)$ as a discontinuous finite element space defined on the macro-partition $\mathcal{M}_h$. The restriction of D_h on a macro-element $M \in \mathcal{M}_h$ is denoted by $D_h(M) := \{v_h|_M \,;\, v_h \in D_h\}$.

The next ingredient is a local projection $\pi_M : L^2(M) \to D_h(M)$ which defines the global projection $\pi_h : L^2(\Omega) \to D_h$ by $(\pi_h v)|_M := \pi_M(v|_M)$ for all $M \in \mathcal{M}_h$. A standard variant is the local orthogonal L^2 projection. Denoting the identity on $L^2(\Omega)$ by id, the associated fluctuation operator $\kappa_h : L^2(\Omega) \to L^2(\Omega)$ is defined by $\kappa_h := id - \pi_h$.

The second approach, the one-level variant, consists in choosing a discontinuous lower order finite element space D_h on the original mesh $\mathcal{T}_h$. The same abstract framework as in the first approach can be used by setting $\mathcal{M}_h = \mathcal{T}_h$.

For both variants, the stabilized discrete formulation reads: find $u_h \in V_{h,k}$ such that

$$a(u_h, v_h) + s_h(u_h, v_h) = (f, v_h)_\Omega, \qquad \forall v_h \in V_{h,k}, \tag{2.4}$$

where the additional stabilization term is given by

$$s_h(u_h, v_h) := \sum_{M \in \mathcal{M}_h} \tau_M (\kappa_h (\boldsymbol{b} \cdot \nabla u_h), \kappa_h (\boldsymbol{b} \cdot \nabla v_h))_M. \tag{2.5}$$

REMARK 2. *The LPS scheme (2.4) with (2.5) will be denoted as streamline-derivative-based LPS scheme (SD-based LPS scheme for short below). Another variant is to replace* $s_h(\cdot,\cdot)$ *with*

$$\tilde{s}_h(u_h, v_h) := \sum_{M \in \mathcal{M}_h} \tilde{\tau}_M (\kappa_h \nabla u_h, \kappa_h \nabla v_h)_M.$$

Later on, it will be called gradient-based LPS scheme. We will summarize the corresponding result in Remark 6.

The constants τ_M and $\tilde{\tau}_M$ will be determined later based on an a priori estimate. Please notice that the stabilizations s_h and $\tilde{s}_h$ act solely on the small scales. Of course, there is some more freedom in the choice of s_h, see also [19, 4].

In order to control the consistency error of the κ_h-dependent stabilization terms, the space D_h has to be large enough; more precisely:

ASSUMPTION 2. *The fluctuation operator* κ_h *satisfies for* $0 \le l \le k$ *the following approximation property:*

$$\exists\, C_\kappa > 0 \ : \qquad \|\kappa_h q\|_{0,M} \le C_\kappa \frac{h_M^l}{k^l} |q|_{l,M}, \quad \forall q \in L^2(\Omega), q|_M \in H^l(M),\ \forall M \in \mathcal{M}_h. \tag{2.6}$$

The subsequent numerical analysis takes advantage of the inverse inequality (see [11])

$$\exists\, \mu_{inv} \ : \quad |v_h|_{1,T} \leq \mu_{inv} k^2 h_T^{-1} \|v_h\|_{0,T}, \quad \forall T \in \mathcal{T}_h, \ \forall v_h \in V_{h,k} \tag{2.7}$$

and of the interpolation properties of the finite element space $V_{h,k}$. For the Scott-Zhang quasi-interpolant operator $I_{h,k}$ [25], one obtains for $v \in V$ with $v|_{\omega_T} \in H^r(\omega_T)$, $r \geq 1$, on the patches $\omega_T := \bigcup_{\overline{T'}\cap\overline{T}\neq\emptyset} T'$

$$\exists\, C > 0 \ : \quad \|v - I_{h,k}v\|_{m,T} \leq C \frac{h_T^{l-m}}{k^{r-m}} \|v\|_{r,\omega_T}, \quad 0 \leq m \leq l = \min\{k+1, r\}. \tag{2.8}$$

The constant C may depend on r.

2.3. Special interpolation operator. Following [19], we construct a special interpolation $j_h : V \to V_{h,k}$ such that the error $v - j_h v$ is L^2-orthogonal to D_h for all $v \in V$. In order to conserve the standard approximation properties, we additionally assume

ASSUMPTION 3. *There exists a constant $\beta > 0$ such that, for any $M \in \mathcal{M}_h$,*

$$\inf_{q_h \in D_h(M)} \sup_{v_h \in Y_h(M)} \frac{(v_h, q_h)_M}{\|v_h\|_{0,M} \|q_h\|_{0,M}} \geq \beta x \tag{2.9}$$

where $Y_h(M) := \{v_h|_M \ ; \ v_h \in V_{h,k}, v_h = 0$ on $\Omega \setminus M\}$.

REMARK 3. *The inf-sup condition (2.9) implies that the space D_h must not be too rich. On the other hand, D_h must be rich enough to fulfil the approximation property (2.6) . Later we will present several function spaces D_h satisfying (2.9).*

LEMMA 2.1. *Let Assumption 3 be satisfied. Then there is an interpolation operator $j_h : V \to V_{h,k}$ such that*

$$(v - j_h v, q_h)_\Omega = 0, \ \ \forall q_h \in D_h, \forall v \in V, \tag{2.10}$$

$$\|v - j_h v\|_{0,M} + \frac{h_M}{k^2} |v - j_h v|_{1,M} \lesssim \left(1 + \frac{1}{\beta}\right) \frac{h_M^l}{k^l} \|v\|_{l,\omega_M},$$
$$\forall M \in \mathcal{M}_h, \quad v \in V \cap H^l(\Omega), \quad 1 \leq l \leq k+1. \tag{2.11}$$

Proof. We follow the lines of the proof of Th. 2.2 in [19], but we take into account the dependence of the constants on the polynomial order and the inf-sup constant β.

Consider any $M \in \mathcal{M}_h$ and define the linear continuous operator $B_h : Y_h(M) \to D_h(M)'$ by

$$\langle B_h v_h, q_h \rangle := (v_h, q_h)_M, \qquad \forall v_h \in Y_h(M), q_h \in D_h(M).$$

Denote $W_h(M) := Ker(B_h)$ and let $W_h(M)^\perp$ be the orthogonal complement of $W_h(M)$ in $Y_h(M)$ with respect to $(\cdot,\cdot)_M$. The Closed Range Theorem yields via Assumption 3 (cf. [12], p. 58, Lemma 4.1) that B_h is an isomorphism from $W_h(M)^\perp$ onto $D_h(M)'$ with $\beta \|v_h\|_{0,M} \leq \|B_h v_h\|_{D_h(M)'}$ for any $v_h \in W_h(M)^\perp$. Therefore, for any $v \in V$, there exists a unique $z_h(v,M) \in W_h(M)^\perp$ with $\|z_h(v,M)\|_{0,M} \leq \frac{1}{\beta}\|v - I_{h,k}v\|_{0,M}$ such that

$$\langle B_h z_h(v,M), q_h \rangle = (z_h(v,M), q_h)_M = (v - I_{h,k}v, q_h)_M, \quad \forall q_h \in D_h(M).$$

Since $\mathcal{M}_h$ is a partition of Ω, we can define an operator $j_h : V \to V_{h,k}$ by $(j_h v)|_M := (I_{h,k}v)|_M + z_h(v,M)$, $M \in \mathcal{M}_h$. Then we immediately obtain the orthogonality property

(2.10). Due to (2.8) the operator j_h satisfies for $1 \le l \le k+1$ and all $M \in \mathcal{M}_h$, $v \in V \cap H^l(\Omega)$

$$\|v - j_h v\|_{0,M}^2 \le \left(1 + \frac{1}{\beta}\right)^2 \|v - I_{h,k} v\|_{0,M}^2 \le C \left(1 + \frac{1}{\beta}\right)^2 \sum_{\substack{T \subset M \\ T \in \mathcal{T}_h}} \frac{h_T^{2l}}{k^{2l}} \|v\|_{l,\omega_T}^2.$$

To derive an approximation property in the H^1 seminorm, we first use the inverse inequality (2.7) and the assumption (2.3), which implies

$$|z_h(v,M)|_{1,M}^2 \le \sum_{\substack{T \subset M \\ T \in \mathcal{T}_h}} \mu_{inv}^2 k^4 h_T^{-2} \|z_h(v,M)\|_{0,T}^2 \lesssim \frac{\mu_{inv}^2}{\beta^2} k^4 h_M^{-2} \|v - I_{h,k} v\|_{0,M}^2.$$

Then, applying the approximation property (2.8), we get

$$\begin{aligned} |v - j_h v|_{1,M} &= |v - I_{h,k} v - z_h(v,M)|_{1,M} \le |v - I_{h,k} v|_{1,M} + |z_h(v,M)|_{1,M} \\ &\lesssim \left(\frac{1}{k} + \frac{\mu_{inv}}{\beta}\right) \frac{h_M^{l-1}}{k^{l-2}} \|v\|_{l,\omega_M}. \end{aligned}$$

□

REMARK 4. *(i) The estimate of Lemma 2.1 is optimal with respect to h_M. The estimate in the seminorm $|\cdot|_{1,M}$ is seemingly sub-optimal regarding k. A discussion of the stability constant β appearing in Lemma 2.1 is given in [21].*
(ii) If $v \in V \cap H^t(\Omega)$ with $t > \frac{3}{2}$, it is possible to replace the Scott-Zhang quasi-interpolant operator $I_{h,k}$ in (2.8) *by a pointwise interpolant, e.g., the Lagrangian interpolant. This allows to replace the sets ω_M in* (2.11) *and in the a priori estimates of the next section by the macro-elements M, see [20].*

3. A priori analysis. The next goal is an error estimate for the scheme (2.4). Therefore, further assumptions on the finite element spaces $V_{h,k}$ and D_h are required. We will derive all results for the SD-based LPS scheme. The corresponding results for the gradient-based LPS scheme, see Remark 2, will be summarized in Remark 6.

3.1. Stability. First, the stability of the scheme will be proven in the mesh-dependent norm

$$|||v||| := \left(\varepsilon |v|_{1,\Omega}^2 + \sigma \|v\|_{0,\Omega}^2 + s_h(v,v)\right)^{\frac{1}{2}}, \qquad \forall v \in V.$$

The corresponding norm for the gradient-based LPS scheme follows by replacing s_h with $\tilde{s}_h$.

LEMMA 3.1. *The following a priori estimate is valid for the SD-based LPS scheme*

$$\varepsilon |u_h|_{1,\Omega}^2 + \sigma \|u_h\|_{0,\Omega}^2 \le |||u_h|||^2 \le (f, u_h)_\Omega, \tag{3.1}$$

hence existence and uniqueness of $u_h \in V_{h,k}$ in the scheme (2.4) follow.

Proof. For any $v \in V$, integration by parts yields $(\boldsymbol{b} \cdot \nabla v, v)_\Omega = -\frac{1}{2}((\nabla \cdot \boldsymbol{b}) v, v)_\Omega = 0$ and therefore

$$(a + s_h)(v,v) = \varepsilon |v|_{1,\Omega}^2 + \sigma \|v\|_{0,\Omega}^2 + s_h(v,v) = |||v|||^2, \quad \forall v \in V. \tag{3.2}$$

This implies (3.1), hence existence and uniqueness of $u_h \in V_{h,k}$ in the scheme (2.4). □

3.2. Approximate Galerkin orthogonality. In LPS methods the Galerkin orthogonality is not fulfilled and a careful analysis of the consistency error has to be done.

LEMMA 3.2. *Let $u \in V$ and $u_h \in V_{h,k}$ be the solutions of (2.1) and of (2.4), respectively. Then, there holds*

$$a(u - u_h, v_h) = s_h(u_h, v_h), \qquad \forall v_h \in V_{h,k}. \tag{3.3}$$

Proof. The assertion (3.3) follows by subtracting (2.4) from (2.1) with $v = v_h$. ◻

Now we estimate the consistency error.

LEMMA 3.3. *Let Assumption 2 be fulfilled and let $u \in V$ with $\boldsymbol{b} \cdot \nabla u \in H^l(M)$ for some $l \in \{0, \dots, k\}$ and for all $M \in \mathcal{M}_h$. Then, there holds for the SD-based LPS scheme*

$$|s_h(u, v_h)| \lesssim \left(\sum_{M \in \mathcal{M}_h} C_M^s \frac{h_M^{2l}}{k^{2l}} |\boldsymbol{b} \cdot \nabla u|_{l,M}^2 \right)^{\frac{1}{2}} |||v_h|||, \qquad \forall v_h \in V_{h,k}$$

with

$$C_M^s := \min \left\{ \tau_M, \frac{(\tau_M \|\boldsymbol{b}\|_{[L^\infty(M)]^d} k^2)^2}{\sigma \, h_M^2} \right\}. \tag{3.4}$$

Proof. Consider any $M \in \mathcal{M}_h$ and $v_h \in V_{h,k}$. Then the Cauchy-Schwarz inequality and Assumption 2 yield

$$(\kappa_h(\boldsymbol{b} \cdot \nabla u), \kappa_h(\boldsymbol{b} \cdot \nabla v_h))_M \lesssim \frac{h_M^l}{k^l} |\boldsymbol{b} \cdot \nabla u|_{l,M} \|\kappa_h(\boldsymbol{b} \cdot \nabla v_h)\|_{0,M}.$$

Furthermore, we deduce using the L^2 stability of κ_h in Assumption 2, the inverse inequality (2.7) and the assumption (2.3) that

$$\|\kappa_h(\boldsymbol{b} \cdot \nabla v_h)\|_{0,M} \lesssim \|\boldsymbol{b}\|_{[L^\infty(M)]^d} |v_h|_{1,M} \lesssim \|\boldsymbol{b}\|_{[L^\infty(M)]^d} k^2 h_M^{-1} \|v_h\|_{0,M}.$$

Thus,

$$\begin{aligned} &\tau_M (\kappa_h(\boldsymbol{b} \cdot \nabla u), \kappa_h(\boldsymbol{b} \cdot \nabla v_h))_M \\ &\qquad \lesssim \sqrt{C_M^s} \frac{h_M^l}{k^l} |\boldsymbol{b} \cdot \nabla u|_{l,M} \left(\sigma \|v_h\|_{0,M}^2 + \tau_M \|\kappa_h(\boldsymbol{b} \cdot \nabla v_h)\|_{0,M}^2 \right)^{\frac{1}{2}}, \end{aligned}$$

which proves the lemma. ◻

3.3. A priori error estimate. The a priori estimate can be proven using the standard technique of combining the stability and the consistency results of the previous subsections.

THEOREM 3.4. *Let $u \in V$ be the solution of (2.1) and $u_h \in V_{h,k}$ the solution of (2.4). We assume that $u \in H^{l+1}(\Omega)$ for some $l \in \{1, \dots, k\}$ and that $\boldsymbol{b} \cdot \nabla u \in H^l(M)$ for all $M \in \mathcal{M}_h$. Furthermore let Assumptions 2 and 3 for the coarse space D_h be satisfied. Then, there holds for the SD-based LPS scheme*

$$|||u - u_h|||^2 \lesssim \sum_{M \in \mathcal{M}_h} \left\{ C_M^s \frac{h_M^{2l}}{k^{2l}} |\boldsymbol{b} \cdot \nabla u|_{l,M}^2 + \left(1 + \frac{1}{\beta}\right)^2 C_M \frac{h_M^{2l}}{k^{2l-2}} \|u\|_{l+1,\omega_M}^2 \right\} \tag{3.5}$$

with C_M^s defined in (3.4) *and*

$$C_M := \varepsilon + \sigma \frac{h_M^2}{k^4} + \frac{h_M^2}{\tau_M k^4} + \tau_M \|\boldsymbol{b}\|_{[L^\infty(M)]^d}^2.$$

Proof. The error is split into $u - u_h = (u - j_h u) + (j_h u - u_h)$. We start with the approximation error $u - j_h u$. Lemma 2.1 yields

$$|||u - j_h u||| \lesssim \left(1 + \frac{1}{\beta}\right) \left(\sum_{M \in \mathcal{M}_h} \left[\varepsilon + \sigma \frac{h_M^2}{k^4} + \tau_M \|\boldsymbol{b}\|^2_{[L^\infty(M)]^d} \right] \frac{h_M^{2l}}{k^{2l-2}} \|u\|^2_{l+1,\omega_M} \right)^{\frac{1}{2}}.$$

Now we estimate the remaining part $w_h := j_h u - u_h$ using (3.2)

$$\begin{aligned} |||j_h u - u_h||| &= \frac{(a + s_h)(j_h u - u_h, w_h)}{|||w_h|||} \\ &= \frac{(a + s_h)(u - u_h, w_h)}{|||w_h|||} + \frac{(a + s_h)(j_h u - u, w_h)}{|||w_h|||} =: I + II. \end{aligned}$$

Applying Lemmata 3.2 and 3.3, the first term is bounded by

$$I = \frac{s_h(u, w_h)}{|||w_h|||} \lesssim \left(\sum_{M \in \mathcal{M}_h} C_M^s \frac{h_M^{2l}}{k^{2l}} |\boldsymbol{b} \cdot \nabla u|^2_{l,M} \right)^{\frac{1}{2}}.$$

Now we consider the terms of II separately. Integration by parts, the orthogonality property (2.10) and the estimate (2.11) yield for $w_h \in V_{h,k}$ that

$$\begin{aligned} a(j_h u - u, w_h) &= \varepsilon(\nabla(j_h u - u), \nabla w_h)_\Omega - (\kappa_h(\boldsymbol{b} \cdot \nabla w_h), j_h u - u)_\Omega + \sigma(j_h u - u, w_h)_\Omega \\ &\lesssim \left(1 + \frac{1}{\beta}\right) \left(\sum_{M \in \mathcal{M}_h} \left[\varepsilon + \left(\sigma + \frac{1}{\tau_M} \right) \frac{h_M^2}{k^4} \right] \frac{h_M^{2l}}{k^{2l-2}} \|u\|^2_{l+1,\omega_M} \right)^{\frac{1}{2}} |||w_h|||. \end{aligned}$$

The estimate of the stabilization term follows using (2.6) and (2.11)

$$s_h(j_h u - u, w_h) \lesssim \left(1 + \frac{1}{\beta}\right) \left(\sum_{M \in \mathcal{M}_h} \tau_M \|\boldsymbol{b}\|^2_{[L^\infty(M)]^d} \frac{h_M^{2l}}{k^{2l-2}} \|u\|^2_{l+1,\omega_M} \right)^{\frac{1}{2}} |||w_h|||.$$

Summing up all inequalities in this proof gives the assertion. □

3.4. Parameter design. Now we will calibrate the stabilization parameters τ_M with respect to the local mesh size h_M, the polynomial degree k of the discrete ansatz functions and problem data. The parameters τ_M are determined by balancing the terms $\frac{h_M^2}{\tau_M k^4} \sim \tau_M \|\boldsymbol{b}\|^2_{[L^\infty(M)]^d}$ in C_M on the right-hand side of the general a priori error estimate (3.5), hence

$$\tau_M \sim \frac{h_M}{\|\boldsymbol{b}\|_{[L^\infty(M)]^d} k^2}. \tag{3.6}$$

Note that the discrete problem is well defined also if $\|\boldsymbol{b}\|_{[L^\infty(M)]^d} = 0$ for some $M \in \mathcal{M}_h$ since

$$|s_h(v, w)| \lesssim \sum_{M \in \mathcal{M}_h} \tau_M \|\boldsymbol{b}\|^2_{[L^\infty(M)]^d} |v|_{1,M} |w|_{1,M}, \qquad \forall v, w \in V.$$

COROLLARY 3.1. *If τ_M satisfies (3.6), then we obtain for the SD-based LPS scheme under the assumptions of Theorem 3.4*

$$|||u-u_h|||^2 \lesssim \sum_{M\in\mathcal{M}_h} \left\{ \frac{h_M^{2l}}{k^{2l}} \min\left\{ \frac{h_M}{k^2}\frac{|\boldsymbol{b}\cdot\nabla u|_{l,M}^2}{\|\boldsymbol{b}\|_{[L^\infty(M)]^d}}, \frac{|\boldsymbol{b}\cdot\nabla u|_{l,M}^2}{\sigma} \right\} \right. \\ \left. + \left(1+\frac{1}{\beta}\right)^2 \left[\varepsilon + \sigma\frac{h_M^2}{k^4} + \|\boldsymbol{b}\|_{[L^\infty(M)]^d}\frac{h_M}{k^2}\right] \frac{h_M^{2l}}{k^{2l-2}}\|u\|_{l+1,\omega_M}^2 \right\}.$$

REMARK 5. *This result requires some discussion:*

i) For $l=k$ and $\varepsilon \lesssim h_M$, we obtain for the second right-hand side term in Corollary 3.1 the optimal convergence rate $\mathcal{O}(h_M^{k+\frac{1}{2}})$ with respect to h_M.
For the first right-hand side term, the optimal rate is obtained if $\boldsymbol{b}\neq \mathbf{0}$ in $\overline{\Omega}$. If this is not the case but $\sigma>0$, then one gets the suboptimal rate $\mathcal{O}(h_M^k)$. In the case of $\sigma=0$, an additional reduction of the rate may occur.

ii) Due to the non-optimal estimate of the convergence order of the interpolation operator j_h in the H^1 seminorm, these estimates are presumably not optimal with respect to polynomial degree k. Let us assume that in Lemma 2.1 there holds

$$\frac{h_M}{k}|v-j_hv|_{1,M} \lesssim \left(1+\frac{1}{\beta}\right)\frac{h_M^l}{k^l}\|v\|_{l,\omega_M}.$$

A careful check of the proofs leads to

$$\tau_M \sim \frac{h_M}{\|\boldsymbol{b}\|_{[L^\infty(M)]^d}\,k}. \tag{3.7}$$

Then the a priori estimate (3.5) in Theorem 3.4 would be optimal with respect to k too with the possible exception of the factors depending on β. Numerical experiments suggest that the choice (3.7) is correct.

REMARK 6. *The result for the gradient-based LPS-scheme (see Remark 2) corresponding to Corollary 3.1 reads as follows: Assume that $\boldsymbol{b}\in[W^{1,\infty}(\Omega)]^d$, $\sigma>0$ and $u\in H^{l+1}(\Omega)$ for some $l\in\{1,\dots,k\}$. Moreover, let Assumptions 2 and 3 hold. For $\tilde\tau_M \sim h_M\|\boldsymbol{b}\|_{[L^\infty(M)]^d}/k^2$ we obtain for the gradient-based LPS scheme*

$$|||u-u_h|||^2 \lesssim \left(1+\frac{1}{\beta}\right)^2 \\ \times \sum_{M\in\mathcal{M}_h}\left[\varepsilon+\sigma\frac{h_M^2}{k^4}+\frac{h_M^2|\boldsymbol{b}|_{[W^{1,\infty}(M)]^d}^2}{\sigma}+\|\boldsymbol{b}\|_{[L^\infty(M)]^d}\frac{h_M}{k^2}\right]\frac{h_M^{2l}}{k^{2l-2}}\|u\|_{l+1,\omega_M}^2.$$

For $l=k, \varepsilon\lesssim h_M$, we obtain the optimal convergence rate $\mathcal{O}(h_M^{k+\frac{1}{2}})$ with respect to h_M. This estimate is better with respect to h_M than for the SD-based LPS scheme, see Remark 5 (i).

4. Examples of finite element spaces. The paper [19] presents different variants for the choice of the discrete spaces $V_{h,k}$ and D_h using simplicial, quadrilateral and hexahedral elements. There are two basic variants of the LPS methods: the one-level approach for which $\mathcal{M}_h=\mathcal{T}_h$ and the two-level approach for which the mesh $\mathcal{T}_h$ is obtained by refining the mesh $\mathcal{M}_h$, see Fig. 4.1 for $d=2$. In what follows, we describe some details of these two approaches.

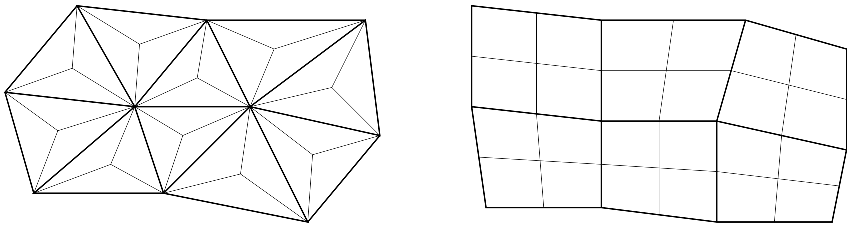

FIG. 4.1. *Relation between the meshes $\mathcal{M}_h$ and $\mathcal{T}_h$ in the two-level approach. The bold lines indicate the mesh $\mathcal{M}_h$, the fine lines $\mathcal{T}_h$*

We shall assume that all macro-elements in $\mathcal{M}_h$ are affine equivalent to the reference element $\hat{T}$ and that $D_h \subset P_{m,\mathcal{M}_h}$ for some $m \in \mathbb{N}_0$. Let us formulate a sufficient condition for the validity of the inf-sup condition (2.9). We introduce a reference bubble function $\hat{b} \in C(\overline{\hat{T}}) \cap H_0^1(\hat{T})$ satisfying $\hat{b} \geq 0$ and $\hat{b} \neq 0$ and, for any $M \in \mathcal{M}_h$, we set $b_M = \hat{b} \circ F_M^{-1}$. Then there exists a positive constant α such that

$$(b_M q, q)_M \geq \alpha \, \|q\|_{0,M}^2, \qquad \forall q \in D_h(M), M \in \mathcal{M}_h.$$

Thus, it suffices to require that

$$b_M \cdot D_h(M) \subset Y_h(M), \qquad \forall M \in \mathcal{M}_h. \tag{4.1}$$

Then the inf-sup condition (2.9) holds with $\beta = (\alpha/\|\hat{b}\|_{L^\infty(\hat{T})})^{1/2}$. Note that a necessary condition for the validity of (2.9) is that $\dim Y_h(M) \geq \dim D_h(M)$. Therefore, if $Y_h(M) = b_M \cdot D_h(M)$, then $Y_h(M)$ has the smallest possible dimension.

The one-level approach with $\mathcal{M}_h = \mathcal{T}_h$ starts from a given discontinuous space D_h and uses an enrichment of the spaces $P_{k,\mathcal{T}_h} \cap V$ or $Q_{k,\mathcal{T}_h} \cap V$ to satisfy (4.1). For simplicial elements, we set

$$D_h := P_{k-1,\mathcal{T}_h}, \qquad V_{h,k} := \{v \in V;\; v|_T \circ F_T \in P_k^{bub}(\hat{T}) \;\forall T \in \mathcal{T}_h\},$$

where

$$P_k^{bub}(\hat{T}) := P_k(\hat{T}) + \hat{b} \cdot P_{k-1}(\hat{T}), \qquad \hat{b}(\hat{x}) := (d+1)^{d+1} \prod_{i=1}^{d+1} \hat{\lambda}_i(\hat{x})$$

with the barycentric coordinates $\hat{\lambda}_i$, $i = 1, \ldots, d+1$. For quadrilateral/hexahedral elements, we can use either $D_h = P_{k-1,\mathcal{T}_h}$ or $D_h = Q_{k-1,\mathcal{T}_h}$. Setting $\hat{D} = P_{k-1}(\hat{T})$ or $\hat{D} = Q_{k-1}(\hat{T})$, respectively, the spaces $V_{h,k}$ are constructed analogously as for simplices with

$$Q_k^{bub}(\hat{T}) := Q_k(\hat{T}) + \hat{b} \cdot \hat{D}, \qquad \hat{b}(\hat{x}) := \prod_{i=1}^{d} (1 - \hat{x}_i^2),$$

where $\hat{T} = (-1,1)^d$. In the numerical experiments presented in the next section, we consider $\hat{D} = Q_{k-1}(\hat{T})$.

Now consider the two-level approach (cf. Figure 4.1 for $d = 2$). In the simplicial case, each element $M \in \mathcal{M}_h$ is devided into $d+1$ simplices by connecting the barycentre of M with the vertices of M. For quadrilateral/hexahedral elements, each $M \in \mathcal{M}_h$ is uniformly refined into 2^d subelements. Then, for simplices, we set

$$V_{h,k} := P_{k,\mathcal{T}_h} \cap V, \qquad D_h := P_{k-1,\mathcal{M}_h}$$

and, for quadrilaterals/hexahedra,

$$V_{h,k} := Q_{k,\mathcal{T}_h} \cap V, \qquad D_h := Q_{k-1,\mathcal{M}_h}.$$

Then the condition (4.1) is obviously satisfied if $\hat{b} \in H_0^1(\hat{T})$ is defined as a nonnegative piecewise P_1/Q_1 function with respect to a division of $\hat{T}$ corresponding to the relation between $\mathcal{M}_h$ and $\mathcal{T}_h$. Hence the inf-sup constant β in Assumption 3 is independent of h. Moreover, the β scales like $\mathcal{O}(\sqrt{k})$ for simplicial elements and like $\mathcal{O}(1)$ for quadrilateral elements in the affine case, see [21].

Note that, for the two-level approach based on simplicial finite elements, the space $V_{h,k}$ can be written in the form

$$V_{h,k} = \{v \in V :\ v|_M \circ F_M \in P_k(\hat{T}) \oplus \hat{B}_k \ \forall M \in \mathcal{M}_h\},$$

where $\hat{B}_k \subset H_0^1(\hat{T})$ is a finite-dimensional space consisting of continuous piecewise polynomial functions of degree k. Therefore, the simplicial two-level approach can be regarded as a one-level approach with respect to the mesh $\mathcal{M}_h$. This will be used in Section 6.

5. Comparison of one- and two-level approach. In this section, we provide a comparison of the one- and two-level variants of the LPS method. The following arguments are relevant for the comparison regarding the efficiency and flexibility:

The data structure for the one-level method is much simpler than for the two-level approach. Moreover, adaptive mesh refinement tools can be easier incorporated. On the other hand, for the same fine mesh, the one-level approach requires more degrees of freedom than the two-level approach.

Moreover, there is a formal argument from the regularity point of view x against the SD-based variant of the two-level method: The assumption $\boldsymbol{b} \cdot \nabla u \in H^l(M)$ for all $M \in \mathcal{M}_h$ in Theorem 3.4 implicitly requires that $\boldsymbol{b} \in [H^l(M)]^d$. This is not realistic as $\boldsymbol{b}$ is usually a finite element solution stemming from a flow simulation. Please note that this argument is not valid for the gradient-based variant of the two-level method.

Now we proceed with the comparison by evaluating some numerical experiments for the SD-based LPS-scheme. First of all, we emphasize that both, the one-level and the two-level method, perform very well according to the theory of Section 3 for problems with solutions without boundary and interior layers. Nevertheless, we omit corresponding results. Here, we concentrate ourselves instead on the more interesting case of problems with layers.

In all numerical experiments, the computational domain Ω is the unit square. We shall consider both one- and two-level approach which will be compared with the SUPG method. The parameter design is $\tau_M = \tau_0 h_M$ for the LPS methods and $\delta_T = \delta_0 h_T$ for the SUPG method with free parameters τ_0 and δ_0. The computations were performed for the one-level method with the Q_1^{bub} and Q_2^{bub} elements on uniform grids consisting of 64×64 and of 32×32 equal square elements, respectively. Similarly, for the SUPG method, we apply the Q_1 and Q_2 elements on uniform grids consisting of 64×64 and of 32×32 equal square elements, respectively. For the two-level approach, we apply the Q_1 and Q_2 elements on uniform grids consisting of 128×128 and of 64×64 equal square elements, respectively. Thus, the corresponding coarse meshes $\mathcal{M}_h$ consist of 64×64 and of 32×32 elements and hence are the same as for the one-level approach. This gives an almost fair comparison of both approaches.

We start with two rather academic problems where the flow field $\boldsymbol{b}$ is aligned with the uniform (Cartesian) mesh in Ω.

EXAMPLE 1. *Exponential outflow layer (see [20], Example 4.2).* *Consider in $\Omega = (0,1)^2$ the model problem (1.1) with $\varepsilon = 10^{-7}$, $\boldsymbol{b} = (0,2)^T$ and $\sigma = 0$. The exact solution*

$$u(x) = (2x_1 - 1)\frac{1 - \exp(-2(1-x_2)/\varepsilon)}{1 - \exp(-2/\varepsilon)}$$

has an exponential boundary layer at the outflow part of the boundary and generates the right-hand side $f = Lu$. On the whole boundary of Ω, a Dirichlet boundary condition determined by u is prescribed. Note that the limit solution $\lim_{\varepsilon\to 0} u(x) = 2x_1 - 1$ can be exactly interpolated by Q_k elements, $k \geq 1$.

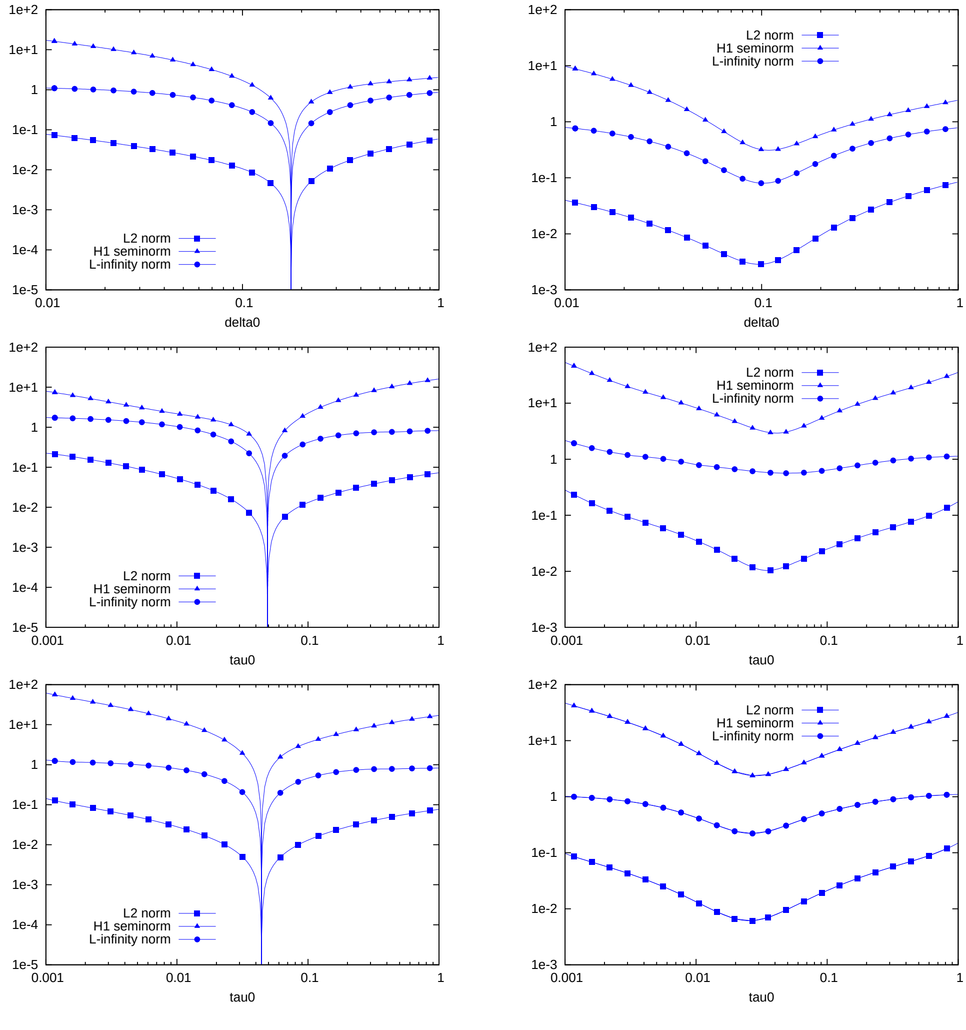

FIG. 5.1. *Dependence of errors on scaling parameters δ_0 and τ_0 for different methods and Example 1: Q_1 elements (left column) and Q_2 elements (right column) for SUPG method (first row), one-level LPS method (second row) and two-level LPS method (third row)*

Figure 5.1 provides a comparison of the errors in the L^2 norm, H^1 seminorm and the (discrete) L^∞ norm vs. the scaling parameters τ_0 for the LPS method and δ_0 for the SUPG method. We calculate all (semi)norms on the subdomain Ω_0 which does not contain those

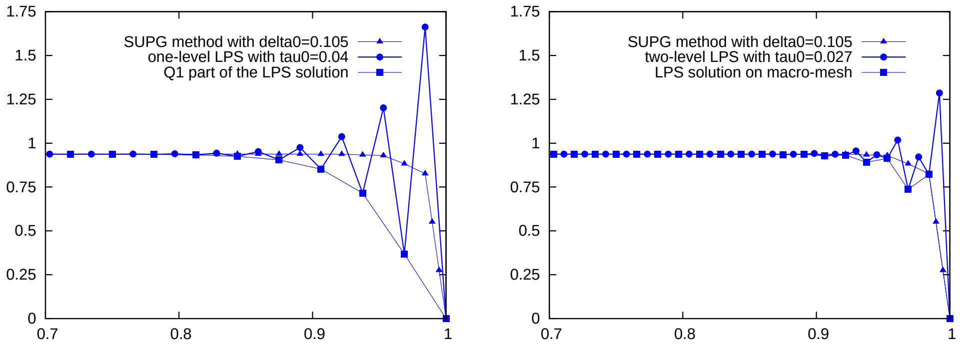

FIG. 5.2. *Cross-section of the discrete solutions for Example 1 at $x_1 = 1 - 1/32$ for one-level method with Q_2^{bub} elements (left) and two-level method with Q_2 elements (right) compared to the SUPG solution*

elements $M \in \mathcal{M}_h$ which intersect the outflow boundary layer at $x_2 = 1$. In particular, the H^1 seminorm of u on these elements would otherwise dominate the error. For the Q_1^{bub} and Q_2^{bub} elements, we drop the additional bubble functions when computing the errors.

First let us consider the Q_1 and Q_1^{bub} elements in the left column of Figure 5.1. For all methods, one observes a global minimum of the errors for some τ_0^* and δ_0^*, which corresponds to the nodally exact solution on Ω resp. Ω_0 in case of the two-level method. The two-level solution possesses a spurious oscillation along $x_2 = 1 - 1/128$ which is in agreement with the one-dimensional theoretical investigations of [23].

The results are less good for the Q_2 and Q_2^{bub} elements in the right column of Figure 5.1 as nodally exact discrete solutions cannot be obtained. Nevertheless, a global minimum can be observed for certain values of τ_0^* and δ_0^*. The LPS methods are clearly outperformed by the SUPG method with the optimized parameter δ_0^*. Furthermore, we observe that the one-level method leads to larger errors with repect to all norms than the two-level method. In particular, the one-level method leads to larger oscillations than the two-level method. This is highlighted by Figure 5.2 where a cross-section of the discrete solutions at $x_1 = 1 - 1/32$ is shown (here the largest oscillations of the discrete solution can be observed). The solutions are shown only for $x_2 \geq 0.7$ since they are nearly constant for $x_2 < 0.7$. It can also be seen that the discrete solutions can be improved if they are replaced by the piecewise bilinear interpolate in case of the one-level method and by the piecewise biquadratic interpolate on the macro-mesh in case of the two-level method. Figure 5.2 further shows the SUPG solution which is signifantly better than both LPS solutions although much less degrees of freedom are needed.

In the above comparison, the number of degrees of freedom considered for the one-level method is smaller than for the two-level method, which leads to a larger smearing of the boundary layer in case of the one-level method, see Figure 5.2. If we apply the one-level method on the fine mesh of the two-level method (and hence the number of degrees of freedom is larger for the one-level method than for the two-level method), than the smearings caused by both LPS methods are comparable but the oscillations of the one-level solutions remain larger than for the two-level method. Also the errors considered in Figure 5.1 remain larger for the one-level method.

EXAMPLE 2. *Parabolic layers (see [20], Example 4.4).*
Consider in $\Omega = (0,1)^2$ *the model problem (1.1) with* $\varepsilon = 10^{-7}$, $\boldsymbol{b} = (0, 1 + x_1^2)^T$, $\sigma = 0$ *and* $f = 0$. *At the outflow boundary* $\Gamma_{out} = (0,1) \times \{1\}$, *a homogeneous Neumann condition is considered whereas, at* $\partial\Omega \setminus \Gamma_{out}$, *an inhomogeneous Dirichlet condition* $u(x) = 1 - x_2$

is prescribed. The exact solution exhibites parabolic layers at $x_1 = 0$ and $x_1 = 1$.

As an exact solution is not available, we provide a comparison of cross-sections of the discrete solution at the outflow part of the boundary at $x_2 = 1$ for different values of τ_0.

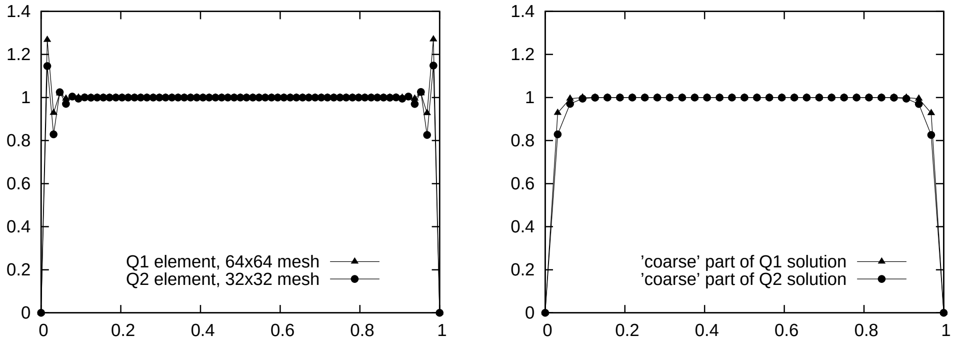

FIG. 5.3. *Outflow profiles for the Galerkin solutions of Example 2*

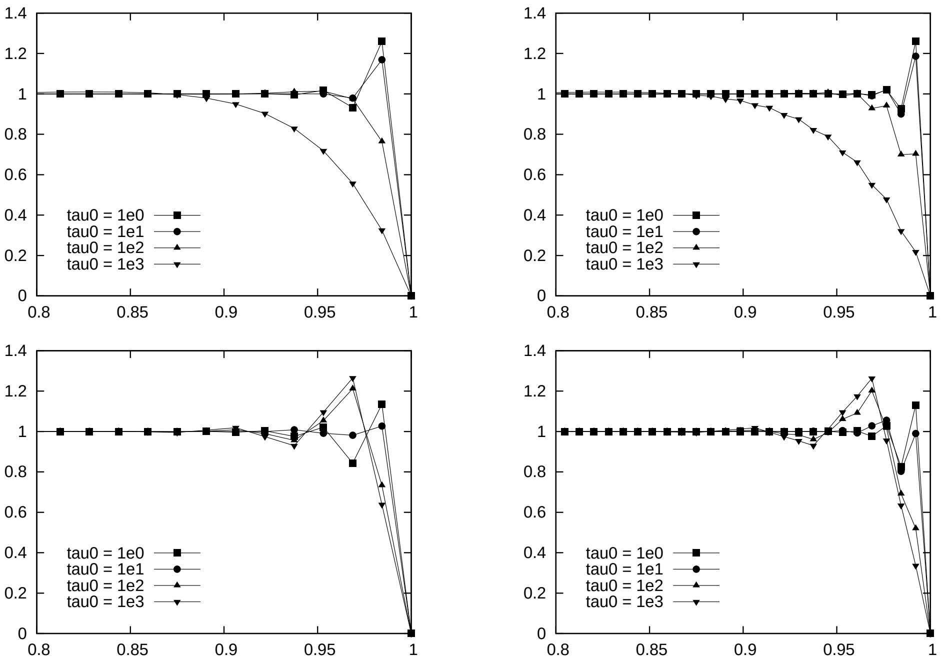

FIG. 5.4. *Outflow profiles for LPS solutions of Example 2 with different values of τ_0: one-level LPS (left column) and two-level LPS (right column) for the Q_1^{bub} and Q_1 elements (first row) and for the Q_2^{bub} and Q_2 elements (second row)*

For this example, the Galerkin method leads to solutions with spurious oscillations localized along the boundary layers, see Figure 5.3 left. Moreover, the oscillations depicted in this figure disappear if we represent the discrete solutions by their values at the vertices of the 32×32 mesh, see Figure 5.3 right. This nice behaviour is seemingly an effect of the Cartesian mesh being aligned with the flow field $\boldsymbol{b}$. In what follows, we shall investigate to what extent the Galerkin solutions can be improved by means of the LPS method. We shall present the outflow profiles only in a neighbourhood of the right boundary layer.

For all four LPS methods and $\tau_0 \in (0.01, 1)$, the outflow profiles are very similar to that of the Galerkin method with the Q_1 or Q_2 element on the mesh $\mathcal{T}_h$ of the respective LPS method. For the two-level methods, this is true also for smaller values of τ_0. For the one-level methods, the behaviour for $\tau_0 \in (0, 0.01)$ is different since the Galerkin solutions for the Q_1^{bub} or Q_2^{bub} elements significantly differ from the Galerkin solutions for the Q_1 or Q_2 elements, respectively.

For $\tau_0 > 10^3$, the LPS with the Q_1 element leads to very similar outflow profiles as the LPS with the Q_1^{bub} element, and the LPS with the Q_2 element gives almost the same outflow profiles as the the LPS with the Q_2^{bub} element. However, the qualitative behaviour of the first order and the second order LPS methods is different. Whereas, for the second order LPS methods, the outflow profiles are basically independent of $\tau_0 > 10^3$, the first order LPS methods introduce a considerable smearing of the boundary layers which increases with increasing τ_0 and makes the discrete solutions useless.

It remains to discuss the properties of the LPS methods for $\tau_0 \in (1, 10^3)$, see Figure 5.4. As we observe, for first order LPS methods, the oscillations decrease with increasing τ_0 but simultaneously the boundary layers are smeared. For second order LPS methods, the oscillations first decrease but soon they again start to increase and, for $\tau_0 = 10^2$, they are already larger than for the Galerkin method. Thus, for first order LPS methods, oscillation-free discrete solutions can be obtained only at the prize of smearing the layers. For second order LPS methods, it seems that, for any choice of τ_0, it is not possible to obtain a discrete solution with sufficiently suppressed spurious oscillations.

An alternative way to suppress the spurius oscillations of the LPS solutions is to consider only a 'coarse' part of the solution like in Figure 5.3. However, for the two-level methods, this does not lead to an improvement in comparison with the 'coarse' part of the Galerkin solution. For the one-level methods, a small improvement is possible, nevertheless, it is questionable whether this improvement is worth the increased computational cost. Moreover, it is very sensitive to the choice of τ_0.

Finally, we consider an example where the flow field $\boldsymbol{b}$ is not aligned with the uniform (Cartesian) mesh.

EXAMPLE 3. *Consider in $\Omega = (0,1)^2$ the model problem (1.1) with $\varepsilon = 10^{-7}$, $\boldsymbol{b} = (-x_2, x_1)^T$, $\sigma = 0$ and $f = 0$. At the outflow boundary $\Gamma_{out} = (0,1) \times \{1\}$, a homogeneous Neumann condition is considered whereas, at $\partial\Omega \setminus \Gamma_{out}$, an inhomogeneous Dirichlet condition $u(x) = 1$ for $x \in [\frac{1}{3}, \frac{2}{3}] \times \{0\}$ and $u(x) = 0$ elsewhere is prescribed. The exact solution exhibits interior parabolic layers starting from the discontinuities of the inflow profile at $x_2 = 0$.*

The solutions of all four LPS methods with optimized parameters τ_0 are comparable, see Figure 5.5 where two such solutions are shown. The discrete solutions detect the interior layers well but have local spurious oscillations in this numerical layers. A comparison of the results for the LPS methods to the SUPG method (not shown) clarifies that the LPS methods cannot outperform the SUPG method.

Summarizing, both variants of the LPS method give comparable results for problems with boundary and interior layers and we have not found any convincing arguments for prefering one of these variants. All methods are able to detect boundary and interior layers numerically but they are rather sensitive to the scaling of the stabilisation parameter. In general, the LPS methods do not attain the quality of the classical SUPG method. As for the SUPG method, the discrete solutions exhibit local spurious oscillations in layer regions unless the mesh is aligned with the advection direction. A potential remedy in case of boundary layers is the weak imposition of Dirichlet data by using Nitzsche's method, cf., e.g., [2]. Another

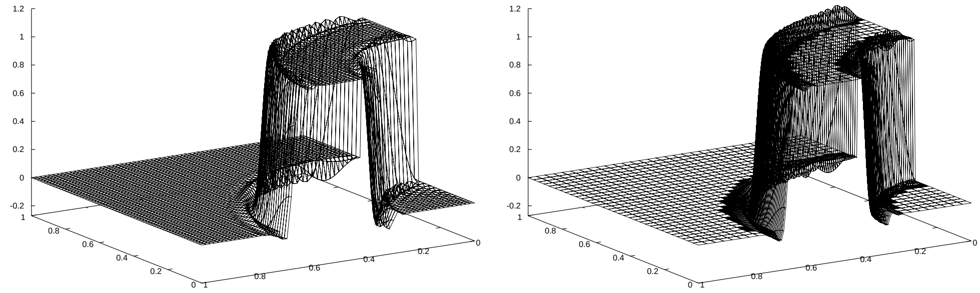

FIG. 5.5. *Plot of the discrete solutions for Example 3 for the one-level method with the* Q_1^{bub} *element and* $\tau_0 = 0.03$ *(left) and for the two-level method with the* Q_2 *element and* $\tau_0 = 3$ *(right)*

idea is the implementation of additional (nonlinear) stabilisation terms which reduce oscillations in crosswind directions around layers, see [17]. Moreover, we refer to the possibility to resolve layers with well-adapted anisotropic finite elements, see, e.g., [18].

6. Relation to residual-based stabilizations. In this section we shall demonstrate that LPS methods based on simplicial meshes are very close to RBS techniques. The dependence on the polynomial degree k will not be considered here.

As we have seen in Section 4, for both the one- and two-level approach, the spaces $V_{h,k}$ and D_h are given by

$$V_{h,k} = \overline{V}_{h,k} \oplus B_{h,k}, \qquad D_h = P_{k-1,\mathcal{M}_h},$$

where

$$\overline{V}_{h,k} := P_{k,\mathcal{M}_h} \cap V, \qquad B_{h,k} := \bigoplus_{M \in \mathcal{M}_h} B_k(M).$$

The spaces $B_k(M)$ are defined using a finite-dimensional space $\hat{B}_k \subset C(\overline{\hat{T}}) \cap H_0^1(\hat{T})$ such that $\hat{B}_k \cap P_k(\hat{T}) = \{0\}$, i.e., for any $M \in \mathcal{M}_h$, we set $B_k(M) := \{\hat{v} \circ F_M^{-1}\,;\ \hat{v} \in \hat{B}_k\}$. Then $B_k(M) \subset H_0^1(M)$ and $B_k(M) \cap P_k(M) = \{0\}$.

Let us consider the gradient-based LPS scheme, i.e., the discrete solution is a function $u_h \in V_{h,k}$ satisfying

$$a(u_h, v_h) + \sum_{M \in \mathcal{M}_h} \tau_M (\kappa_h \nabla u_h, \kappa_h \nabla v_h)_M = (f, v_h)_\Omega, \qquad \forall v_h \in V_{h,k}, \tag{6.1}$$

where we dropped the tilde over τ_M for simplicity. The local projection $\pi_M : L^2(M) \to D_h(M) = P_{k-1}(M)$ used to define the fluctuation operator κ_h is assumed to be the orthogonal L^2 projection of $L^2(M)$ onto $P_{k-1}(M)$. We shall also use the local fluctuation operator $\kappa_M := id - \pi_M$. Note that, for any $\overline{v}_h \in \overline{V}_{h,k}$, we have $\nabla \overline{v}_h \in [D_h]^d$ and hence $\kappa_h \nabla \overline{v}_h = \mathbf{0}$. Thus, it follows from (6.1) that

$$a(u_h, \overline{v}_h) = (f, \overline{v}_h)_\Omega, \qquad \forall \overline{v}_h \in \overline{V}_{h,k}. \tag{6.2}$$

We define the bilinear forms

$$a_M(u, v) := \varepsilon(\nabla u, \nabla v)_M + (\boldsymbol{b} \cdot \nabla u, v)_M + \sigma(u, v)_M,$$
$$a_M^\star(u, v) := \varepsilon(\nabla u, \nabla v)_M - (\boldsymbol{b} \cdot \nabla u, v)_M + \sigma(u, v)_M.$$

Then

$$a_M(u,v) = a_M^\star(v,u), \qquad \forall u,v \in H_0^1(M), M \in \mathcal{M}_h. \tag{6.3}$$

Denoting

$$L^\star u := -\varepsilon\Delta u - \boldsymbol{b}\cdot\nabla u + \sigma u,$$

we have

$$a_M(u,v) = (Lu,v)_M, \qquad \forall u \in H^2(M), v \in H_0^1(M), \tag{6.4}$$
$$a_M(u,v) = (u,L^\star v)_M, \qquad \forall u \in H_0^1(M), v \in H^2(M). \tag{6.5}$$

Using the local bilinear forms, we deduce from (6.1) that, for any $M \in \mathcal{M}_h$, we have

$$a_M(u_h,v_M) + \tau_M(\kappa_M\nabla u_h, \kappa_M\nabla v_M)_M = (f,v_M)_M, \qquad \forall v_M \in B_k(M). \tag{6.6}$$

We denote by $\overline{u}_h \in \overline{V}_{h,k}$ and $u_h^b \in B_{h,k}$ the uniquely determined functions satisfying $\overline{u}_h + u_h^b = u_h$ and set $u_M = u_h^b|_M$ for any $M \in \mathcal{M}_h$. Combining (6.4) and (6.6), we derive that

$$a_M(u_M,v_M) + \tau_M(\kappa_M\nabla u_M, \kappa_M\nabla v_M)_M = (f - L\overline{u}_h, v_M)_M, \qquad \forall v_M \in B_k(M).$$

We define one-to-one linear operators A_M, $A_M^\star : B_k(M) \to B_k(M)$ by

$$a_M(u,v) + \tau_M(\kappa_M\nabla u, \kappa_M\nabla v)_M = (A_M u, v)_M, \qquad \forall u,v \in B_k(M),$$
$$a_M^\star(v,u) + \tau_M(\kappa_M\nabla v, \kappa_M\nabla u)_M = (u, A_M^\star v)_M, \qquad \forall u,v \in B_k(M).$$

According to (6.3), the operator $A_M^\star$ is adjoint to the operator A_M. Clearly,

$$(A_M u_M, v_M)_M = (f - L\overline{u}_h, v_M)_M, \qquad \forall v_M \in B_k(M)$$

and hence

$$u_M = A_M^{-1}\varrho_M(f - L\overline{u}_h), \tag{6.7}$$

where ϱ_M is the orthogonal L^2 projection from $L^2(M)$ onto $B_k(M)$. According to (6.2), we have

$$a(\overline{u}_h, \overline{v}_h) + \sum_{M\in\mathcal{M}_h} a_M(u_M, \overline{v}_h) = (f, \overline{v}_h)_\Omega, \qquad \forall \overline{v}_h \in \overline{V}_{h,k}.$$

Using (6.5) and (6.7), we obtain

$$a_M(u_M, \overline{v}_h) = (u_M, L^\star\overline{v}_h)_M = (A_M^{-1}\varrho_M(f - L\overline{u}_h), \varrho_M L^\star\overline{v}_h)_M, \qquad \forall \overline{v}_h \in \overline{V}_{h,k}$$

and hence we derive that

$$a(\overline{u}_h, \overline{v}_h) + \sum_{M\in\mathcal{M}_h} (f - L\overline{u}_h, (A_M^\star)^{-1}\varrho_M L^\star\overline{v}_h)_M = (f, \overline{v}_h)_\Omega, \qquad \forall \overline{v}_h \in \overline{V}_{h,k}. \tag{6.8}$$

Since $(A_M^\star)^{-1}$ maps into $B_k(M)$, it is not necessary to apply the projection ϱ_M to $f - L\overline{u}_h$.

The relation (6.8) shows that any simplicial LPS method can be interpreted as a residual-based stabilization. The operator $(A_M^\star)^{-1}$ plays the role of a stabilization parameter and we shall investigate in the following how it depends on the LPS parameter τ_M and on the data of the problem (1.1).

LEMMA 6.1. *There exists* $\gamma > 0$ *such that*

$$\|\kappa_M \nabla v\|_{0,M} \geq \gamma \|\nabla v\|_{0,M}, \qquad \forall v \in B_k(M), M \in \mathcal{M}_h.$$

Proof. Consider any $M \in \mathcal{M}_h$ and $v \in B_k(M)$. Then there exists $\hat{v} \in \hat{B}_k$ such that $v = \hat{v} \circ F_M^{-1}$ and we have $\nabla v = (DF_M)^{-M}(\hat{\nabla}\hat{v}) \circ F_M^{-1}$ where DF_M is the Jacobi matrix of F_M. Thus, given any $i \in \{1, \ldots, d\}$, there exists a vector $\boldsymbol{a} \in \mathbb{R}^d$ such that $(\partial v/\partial x_i) \circ F_M = \boldsymbol{a} \cdot \hat{\nabla}\hat{v}$. Consequently, it suffices to prove the existence of $\gamma > 0$ such that

$$\|\hat{\kappa}(\boldsymbol{a} \cdot \hat{\nabla}\hat{v})\|_{0,\hat{T}} \geq \gamma \|\boldsymbol{a} \cdot \hat{\nabla}\hat{v}\|_{0,\hat{T}}, \qquad \forall \boldsymbol{a} \in \mathbb{R}^d, \hat{v} \in \hat{B}_k, \tag{6.9}$$

where $\hat{\kappa} = id - \hat{\pi}$ and $\hat{\pi}$ is the orthogonal L^2 projection of $L^2(\hat{T})$ onto $P_{k-1}(\hat{T})$. Let us assume that (6.9) does not hold for any $\gamma > 0$. Then there exist sequences $\{\boldsymbol{a}_n\}_{n=1}^\infty \subset \mathbb{R}^d$ and $\{\hat{v}_n\}_{n=1}^\infty \subset \hat{B}_k$ such that $|\boldsymbol{a}_n| = 1$, $\|\hat{\nabla}\hat{v}_n\|_{0,\hat{T}} = 1$ and $\|\hat{\kappa}(\boldsymbol{a}_n \cdot \hat{\nabla}\hat{v}_n)\|_{0,\hat{T}} < (1/n)\|\boldsymbol{a}_n \cdot \hat{\nabla}\hat{v}_n\|_{0,\hat{T}} \leq 1/n$ for any $n \in \mathbb{N}$. Since the spaces $\mathbb{R}^d$ and $\hat{B}_k$ are finite-dimensional, there exist subsequences $\{\boldsymbol{a}_{n_l}\}$ and $\{\hat{v}_{n_l}\}$ converging to some $\boldsymbol{a} \in \mathbb{R}^d$ and $\hat{v} \in \hat{B}_k$, respectively. Clearly, $|\boldsymbol{a}| = 1$, $\|\hat{\nabla}\hat{v}\|_{0,\hat{T}} = 1$ and $\hat{\kappa}(\boldsymbol{a} \cdot \hat{\nabla}\hat{v}) = 0$. The last relation implies that $\boldsymbol{a} \cdot \hat{\nabla}\hat{v} \in P_{k-1}(\hat{T})$ and hence $\hat{v} \in P_k(\hat{T})$ since $\hat{v} \in C(\overline{\hat{T}}) \cap H_0^1(\hat{T})$. Consequently, $\hat{v} = 0$ as $\hat{B}_k \cap P_k(\hat{T}) = \{0\}$. This is in contradiction with the fact that $\|\nabla\hat{v}\|_{0,\hat{T}} = 1$. □

THEOREM 6.2. *There exist positive constants* C_1 *and* C_2 *such that, for any* $M \in \mathcal{M}_h$ *and* $g \in B_k(M)$*, we have*

$$\frac{C_1 h_M^2}{\varepsilon + \tau_M + \|\boldsymbol{b}\|_{[L^\infty(M)]^d} h_M + \sigma h_M^2} \leq \frac{\|(A_M^\star)^{-1} g\|_{0,M}}{\|g\|_{0,M}} \leq \frac{C_2 h_M^2}{\varepsilon + \tau_M + \sigma h_M^2}. \tag{6.10}$$

Proof. Consider any $M \in \mathcal{M}_h$ and $g \in B_k(M)$ and set $u = (A_M^\star)^{-1} g$. Then $a_M^\star(u, v) + \tau_M(\kappa_M \nabla u, \kappa_M \nabla v)_M = (g, v)_M$ for any $v \in B_k(M)$. It is well known that

$$C_3 h_M |v|_{1,M} \leq \|v\|_{0,M} \leq h_M |v|_{1,M}, \qquad \forall v \in B_k(M),$$

where C_3 is positive and independent of M and v. Therefore, in view of Lemma 6.1,

$$\begin{aligned} h_M |u|_{1,M} \|g\|_{0,M} &\geq (g, u)_M = \varepsilon |u|_{1,M}^2 + \sigma \|u\|_{0,M}^2 + \tau_M \|\kappa_M \nabla u\|_{0,M}^2 \\ &\geq (\varepsilon + \gamma^2 \tau_M + \sigma C_3^2 h_M^2) |u|_{1,M}^2, \end{aligned}$$

which implies that

$$\min\{1, \gamma^2, C_3^2\}(\varepsilon + \tau_M + \sigma h_M^2) \|u\|_{0,M} \leq h_M^2 \|g\|_{0,M},$$

thus proving the right-hand side inequality in (6.10). On the other hand, for any $v \in B_k(M)$, we have

$$(g, v)_M \leq \{(\varepsilon + \tau_M) C_3^{-1} h_M^{-1} + \|\boldsymbol{b}\|_{[L^\infty(M)]^d} + \sigma h_M\} |u|_{1,M} \|v\|_{0,M},$$

where we used the fact that $\|\kappa_M z\|_{0,M}^2 = \|z\|_{0,M}^2 - \|\pi_M z\|_{0,M}^2 \leq \|z\|_{0,M}^2$ for any $z \in L^2(M)$. Consequently,

$$C_3^2 h_M^2 \|g\|_{0,M} \leq \max\{1, C_3\}(\varepsilon + \tau_M + \|\boldsymbol{b}\|_{[L^\infty(M)]^d} h_M + \sigma h_M^2) \|u\|_{0,M},$$

which completes the proof. ◻

REMARK 7. *Let us consider the simplest case $k = 1$. Since, for any $M \in \mathcal{M}_h$, the space $B_1(M)$ is one-dimensional, the operator $A_M^\star$ represents a multiplicative factor and we easily obtain*

$$(A_M^\star)^{-1} = \frac{\|b_M\|_{0,M}^2}{(\varepsilon + \tau_M)|b_M|_{1,M}^2 + \sigma \|b_M\|_{0,M}^2},$$

where $b_M = \hat{b} \circ F_M^{-1}$. Moreover, introducing the mean values

$$\boldsymbol{b}_M = \frac{(\boldsymbol{b}, b_M)_M}{(1, b_M)_M}, \qquad f_M = \frac{(f, b_M)_M}{(1, b_M)_M}$$

and denoting by x_M the barycentre of M, we derive that

$$(f - L\overline{u}_h, (A_M^\star)^{-1} \varrho_M L^\star \overline{v}_h)_M = \delta_M (\boldsymbol{b}_M \cdot \nabla \overline{u}_h + \sigma \overline{u}_h - f_M, \boldsymbol{b}_M \cdot \nabla \overline{v}_h - \sigma \overline{v}_h(x_M))_M$$

with

$$\delta_M = \frac{(1, b_M)_M^2}{|M|\{(\varepsilon + \tau_M)|b_M|_{1,M}^2 + \sigma \|b_M\|_{0,M}^2\}},$$

where $|M|$ is the volume of M.

REMARK 8. *Let us consider the SD-based LPS scheme (2.4), (2.5) which we now write in the form*

$$a(u_h, v_h) + \sum_{M \in \mathcal{M}_h} \tau_M (\kappa_h(\boldsymbol{e_b} \cdot \nabla u_h), \kappa_h(\boldsymbol{e_b} \cdot \nabla v_h))_M = (f, v_h)_\Omega, \qquad \forall v_h \in V_{h,k},$$

where $\boldsymbol{e_b} = \boldsymbol{b}/|\boldsymbol{b}|$ ($\boldsymbol{e_b} = \boldsymbol{0}$ if $\boldsymbol{b} = \boldsymbol{0}$). If we assume that $\boldsymbol{b}$ is piecewise constant, we again deduce that the component $\overline{u}_h \in \overline{V}_{h,k}$ of the discrete solution $u_h \in V_{h,k}$ satisfies the relation (6.8), where the operator $A_M^\star : B_k(M) \to B_k(M)$ is now defined by

$$a_M^\star(v, u) + \tau_M (\kappa_M(\boldsymbol{e_b} \cdot \nabla v), \kappa_h(\boldsymbol{e_b} \cdot \nabla u))_M = (u, A_M^\star v)_M, \qquad \forall u, v \in B_k(M).$$

It is easy to check that the statement of Theorem 6.2 remains valid as well, provided that $\tau_M = 0$ if $\boldsymbol{b}|_M = 0$.

REMARK 9. *As we see from (6.10), the limit case $\tau_M \to \infty$ corresponds to the Galerkin discretization (2.2).*

7. Summary. In this paper, we considered the local projection stabilization (LPS) of finite element methods for the linear advection-diffusion-reaction problem. This new technique for the numerical solution of transport-dominated problems preserves the stability and accuracy of methods with residual-based stabilization but has a symmetric form of the stabilization term. We gave a critical discussion and comparison of the one- and two-level approaches to LPS which showed that there are no convincing arguments for prefering one of these approaches. Moreover, the relation between the LPS method and residual-based stabilization techniques was explained for simplical elements.

Acknowledgments. The research of Petr Knobloch is a part of the project MSM 0021620839 financed by MSMT and it was partly supported by the Grant Agency of the Academy of Sciences of the Czech Republic under the grant No. IAA100190804. We thank Benjamin Tews for his numerical experiments for the two-level approach.

REFERENCES

[1] ARNOLD, D., BOFFI, D., AND FALK, R. Approximation by quadrilateral finite elements. *Math. Comp. 71* (2002), 909–922.

[2] BAZILEVS, Y., AND HUGHES, T. Weak imposition of Dirichlet boundary conditions in fluid mechanics, 2007. Technical Report 2007, ICES Austin.

[3] BECKER, R., AND VEXLER, B. Stabilized finite element methods for the generalized Oseen problem. *Numer. Math. 106* (2007), 349–367.

[4] BRAACK, M., AND BURMAN, E. Local projection stabilization for the Oseen problem and its interpretation as a variational multiscale method. *SIAM J. Numer. Anal. 43*, 6 (2006), 2544–2566.

[5] BRAACK, M., BURMAN, E., JOHN, V., AND LUBE, G. Stabilized finite element methods for the generalized Oseen problem. *Comput. Methods Appl. Mech. Engrg. 196* (2007), 853–866.

[6] BROOKS, A., AND HUGHES, T. Streamline upwind/Petrov-Galerkin formulations for convection dominated flows with particular emphasis on the incompressible Navier-Stokes equations. *Comput. Methods Appl. Mech. Engrg. 32* (1982), 199–259.

[7] BURMANN, E., AND HANSBO, P. Edge stabilization for Galerkin approximations of convection-diffusion problems. *Comput. Methods Appl. Mech. Engrg. 193* (2004), 1437–1453.

[8] CODINA, R. Analysis of a stabilized finite element approximation of the Oseen equations using orthogonal subscales. *Appl. Numer. Math. 58* (2008), 264–283.

[9] FRANCA, L., AND VALENTIN, F. On an improved unusual stabilized finite element method for the advective-reactive-diffusive equation. *Comput. Methods Appl. Mech. Engrg. 190* (2000), 1785–1800.

[10] GANESAN, S., AND TOBISKA, L. Stabilization by local projection. Convection-diffusion and incompressible flow problems. Tech. rep., Otto-von-Guericke University Magdeburg, IAN, Preprint 2007-46. to appear in J. Sci. Comput., 2007.

[11] GEORGOULIS, E. Inverse-type estimates on hp-finite element spaces and applications, 2007. to appear in Math. Comput.

[12] GIRAULT, V., AND RAVIART, P. *Finite Element Methods for Navier-Stokes Equations*. Springer, Heidelberg-Berlin, 1986.

[13] GRAVEMEIER, V. The variational multiscale method for laminar and turbulent flow. *Arch. Comput. Methods Engrg. 13* (2006), 249–324.

[14] HUGHES, T. Multiscale phenomena: Green's functions, the Dirichlet-to-Neumann formulation, subgrid scale models, bubbles and the origins of stabilized methods. *Comput. Methods Appl. Mech. Engrg. 127* (1995), 387–401.

[15] HUGHES, T., MAZZEI, L., AND JANSSEN, K. Large eddy simulation and the variational multiscale method. *Comput. Vis. Sci. 3* (2000), 47–59.

[16] JOHN, V., AND KAYA, S. A finite element variational multiscale method for the Navier-Stokes equations. *SIAM J. Sci. Comput. 26* (2005), 1485–1503.

[17] JOHN, V., AND KNOBLOCH, P. On spurious oscillations at layers diminuishing (SOLD) methods for convection-diffusion problems: Part I - A review. *Comput. Methods Appl. Mech. Engrg. 196* (2007).

[18] MADDEN, N., AND STYNES, M. Efficient generation of orientied meshes for solving convection-diffusion problems. *Int. J. Numer. Methods Engrg. 40* (1997).

[19] MATTHIES, G., SKRZYPACZ, P., AND TOBISKA, L. A unified convergence analysis for local projection stabilizations applied to the Oseen problem. M^2AN *41*, 4 (2007), 713–742.

[20] MATTHIES, G., SKRZYPACZ, P., AND TOBISKA, L. Stabilization of local projection type applied to convection-diffusion problems with mixed boundary conditions. Tech. rep., Otto-von-Guericke University Magdeburg, IAN, Preprint 2007-44, 2007.

[21] RAPIN, G., LUBE, G., AND LÖWE, J. Local projection stabilizations for inf-sup stable finite elements applied to the Oseen problem , 2007. to appear in Proc. ENUMATH 2007, Springer 2008.

[22] ROOS, H.-G., STYNES, M., AND TOBISKA, L. *Robust Numerical Methods for Singularly Perturbed Differential Equations*. Springer, Berlin - Heidelberg - New York, 2008.

[23] ROOS, H.-G., AND VANSELOW, R. A comparison of four- and five-point difference approximations for stabilizing the one-dimensional stationary convection-diffusion equation, 2007. Technical Report, TU Dresden.

[24] SCHMALJOHANN, S. Local projection stabilization for the Oseen problem (in German), 2007. Master Thesis, Ruhr-Universität Bochum.

[25] SCOTT, L., AND ZHANG, S. Finite element interpolation of nonsmooth functions satisfying boundary conditions. *Math. Comput. 54* (1990), 483–493.

Institut für Numerische und Angewandte Mathematik
Universität Göttingen
Lotzestr. 16-18
D - 37083 Göttingen

Telefon: 0551/394512
Telefax: 0551/393944

Email: trapp@math.uni-goettingen.de URL: http://www.num.math.uni-goettingen.de

Verzeichnis der erschienenen Preprints 2008:

2008-01	M. Körner, A. Schöbel	Weber problems with high-speed curves
2008-02	S. Müller, R. Schaback	A Newton Basis for Kernel Spaces
2008-03	H. Eckel, R. Kress	Nonlinear integral equations for the complete electrode model in inverse impedance tomography
2008-04	M. Michaelis, A. Schöbel	Integrating Line Planning, Timetabling, and Vehicle Scheduling: A customer-oriented approach
2008-05	O. Ivanyshyn, R. Kress, P. Serranho	Huygen's principle and iterative methods in inverse obstacle scattering
2008-06	F. Bauer, T. Hohage, A. Munk	Iteratively regularized Gauss-Newton method for nonlinear inverse problems with random noise
2008-07	R. Kress, N. Vintonyak	Iterative methods for planar crack reconstruction in semi-infinite domains
2008-08	M. Uecker, T. Hohage, K.T. Block, J. Frahm	Image reconstruction by regularized nonlinear inversion - Joint estimation of coil sensitivities and image content
2008-09	M. Schachtebeck, A. Schöbel	IP-based Techniques for Delay Management with Priority Decisions
2008-10	S. Cicerone, G. Di Stefano, M. Schachtebeck, A. Schöbel	Dynamic Algorithms for Recoverable Robustness Problems
2008-11	M. Braack, G. Lube	Stabilized finite elements by local projection for flow problems
2008-12	T. Knopp, X.Q. Zhang, R. Kessler, G. Lube	Calibration of a finite volume discretization and of model parameters for incompressible large eddy-type simulations
2008-13	P. Knobloch, G. Lube	Local projection stabilization for advection-diffusion-reaction problems: One-level vs. two-level approach